

Experimental validation of a multi-level damage localization technique with distributed computation

Guirong Yan^{1,2}, Weijun Guo³, Shirley J. Dyke^{1*}, Gregory Hackmann³ and Chenyang Lu³

¹*School of Mechanical Engineering, Purdue University, West Lafayette, IN 47907-2021, USA*

²*School of Engineering, University of Western Sydney, Penrith, NSW 1797, Australia*

³*Department of Computer Science and Engineering, Washington University,
Campus Box 1045, St. Louis, MO 63130, USA*

(Received October 14, 2009, Accepted March, 30, 2010)

Abstract. This study proposes a multi-level damage localization strategy to achieve an effective damage detection system for civil infrastructure systems based on wireless sensors. The proposed system is designed for use of distributed computation in a wireless sensor network (WSN). Modal identification is achieved using the frequency-domain decomposition (FDD) method and the peak-picking technique. The ASH (angle-between-string-and-horizon) and AS (axial strain) flexibility-based methods are employed for identifying and localizing damage. Fundamentally, the multi-level damage localization strategy does not activate all of the sensor nodes in the network at once. Instead, relatively few sensors are used to perform coarse-grained damage localization; if damage is detected, only those sensors in the potentially damaged regions are incrementally added to the network to perform finer-grained damage localization. In this way, many nodes are able to remain asleep for part or all of the multi-level interrogations, and thus the total energy cost is reduced considerably. In addition, a novel distributed computing strategy is also proposed to reduce the energy consumed in a sensor node, which distributes modal identification and damage detection tasks across a WSN and only allows small amount of useful intermediate results to be transmitted wirelessly. Computations are first performed on each leaf node independently, and the aggregated information is transmitted to one cluster head in each cluster. A second stage of computations are performed on each cluster head, and the identified operational deflection shapes and natural frequencies are transmitted to the base station of the WSN. The damage indicators are extracted at the base station. The proposed strategy yields a WSN-based SHM system which can effectively and automatically identify and localize damage, and is efficient in energy usage. The proposed strategy is validated using two illustrative numerical simulations and experimental validation is performed using a cantilevered beam.

Keywords: wireless sensor network; damage localization; damage detection; structural health monitoring.

1. Introduction

According to a recent report from the American Society for Civil Engineers, “more than 26%, or one in four, of the nation’s bridges are either structurally deficient or functionally obsolete” (ASCE 2009). Actually, a large percentage of the bridges in use in the United States have been used for several decades, often beyond their intended service lifetime, and their condition should be assessed and monitored during future usage. The collapse of the I-35W highway bridge over the

*Corresponding Author, Professor, E-mail: sdyke@purdue.edu

Mississippi River in Minneapolis (Minnesota, US, August 2007) further underscores the need for reliable and robust structural health monitoring (SHM). With low installation and maintenance expenses, structural health monitoring and damage detection based on wireless sensor networks (WSNs) has attracted much attention. Using a WSN, a dense deployment of measurement points in a structure is possible, which facilitates accurate and fault tolerant damage detection techniques (Nagayama and Spencer 2007).

Although the SHM systems based on WSNs have shown considerable promise (Horton *et al.* 2002, Lynch *et al.* 2002, Spencer 2003, Yu *et al.* 2009, Yu and Ou 2009) for civil infrastructure applications, they present some new technical challenges for real-world applications, such as, energy supply constraints, time synchronization errors (TSEs), limited wireless communication bandwidth, and unreliable wireless communication (Wang *et al.* 2007a). In particular, the limited energy available in each sensor node presents challenges for long-term operation of SHM systems. Schemes for conserving energy to prolong the lifetime of a WSN can be classified into three categories.

- i) Energy harvesting technologies: the concept of energy harvesting was introduced to WSNs to recharge batteries from solar or vibrational energy (Hill 2003, Feng *et al.* 2002).
- ii) Power management techniques: certain protocols may be used to minimize the energy consumption of a node while it is awake. For example, duty cycling protocols like BoX-MAC (Moss and Levis 2008) and SCP (Ye *et al.* 2006) topology control protocols such as ART (Hackmann *et al.* 2008). Alternatively, wireless sensors may be designed to consume very little power in the sleep state, so much so that the energy used to make the sensor active for any reason can be orders of magnitude greater than making the sensor remain asleep (Polastre *et al.* 2005). Therefore, an alternative is to make unused sensors enter a low power sleep mode, and wake up periodically or by event-triggered signals (Galbreath *et al.* 2003).
- iii) Power efficiency by reducing the amount of wireless communication: because wireless communication often consumes the greatest amount of energy among all components in an awakened node, algorithms which require transmission of long time-history records to the central server should be avoided. Power efficiency can be achieved by pre-processing the raw data at each sensor node prior to transmission and then just transmitting small amount of useful results wirelessly.

Because current power harvesting techniques that provide a low-cost, portable solution for WSNs are still under development (Wang *et al.* 2007a), research in power efficiency through distributed computing has received considerable attention. Lynch *et al.* (2004) embedded an algorithm into each wireless sensor to locally process measured raw data to identify AR or ARX coefficients using collected responses, and took the residual error of the AR or ARX model as a damage sensitive feature. The damage detection algorithm, statistical pattern recognition, was employed to perform a statistical analysis on extracted damage features to identify damage. Only the AR or ARX model coefficients were wirelessly transmitted, and therefore, the energy consumed for transmission was considerably reduced. This type of distributed computing strategy for damage detection has also been employed by Chintalapudi *et al.* (2005), although the damage detection algorithm used here was based on detecting frequency shifts caused by damage. However, both methods were only used to identify the existence of damage. To localize damage, Castaneda *et al.* (2008) and Hackmann *et al.* (2008) employed the DLAC method (Messina *et al.* 1996) which is based on a correlation analysis between identified natural frequencies from measured data and analytical ones in each simulated damage pattern. Herein, an FFT algorithm and a curve fitting technique for the power spectral density (PSD) of the response were embedded in the microprocessors of wireless sensors for locating resonant frequencies. Only a small number of curve fit parameters were transmitted wirelessly to the base station for further

identifying natural frequencies and performing the DLAC method. However, the DLAC method has some limitations because it is not applicable to multiple damage scenarios or structures with symmetries. Some other research based on decentralizing the damage detection procedures across a WSN can be referred to (Jeong *et al.* 2009, Wang *et al.* 2007b).

In this study a WSN-based SHM system is developed based on the integrated constraints associated with both accurate damage detection and energy consumption. We implement a modal identification method and flexibility-based damage detection methods using the wireless sensor network. A combination of the last two energy-conserving techniques is used to extend the lifetime of this SHM system. A multi-level damage localization strategy is proposed and experimentally validated. The sensor nodes are activated in the network in stages to improve the efficiency of the network. Relatively few sensors are used to perform coarse-grained damage localization. If damage is detected, only those sensors in potentially damaged regions are incrementally added to the network to perform finer-grained damage localization. Two damage localization methods which are suitable for multi-level damage localization are discussed, which are the ASH (angle-between-string-and-horizon) or AS (axial strain) flexibility-based damage detection methods (Yan *et al.* 2008, 2009). These methods involve both information on mode shapes and natural frequencies and thus can localize multiple damage sites in structures.

The proposed approach is designed to use a distributed computing strategy and uses a multi-level damage detection method. Computations associated with modal identification and damage detection steps are executed across multiple sensor nodes to distribute the computing across the WSN. In this way, the raw data is processed at each sensor node, and minimal amounts of useful intermediate results are transmitted wirelessly. The distributed computing strategy with the same modal identification method was also used in (Zimmerman *et al.* 2008). However, the communication cost and computation cost of the system described in this paper is reduced compared to that in (Zimmerman *et al.* 2008). Rather than transmitting the peaks in the PSD of the response at each sensor node to the next sensor node, having the FDD procedures executed at the next sensor node(s) to obtain partial two-node mode shapes that must be stitched together, we transmit the peaks in the PSD of the response at each sensor node to a common node directly. With less communication involved, it is reasonable to assume that less energy is consumed than in (Zimmerman *et al.* 2008). Additionally there may be advantages in terms of the accuracy of the identified mode shapes. Herein an approach is proposed to implement a two-stage damage detection strategy and numerically demonstrated using a cantilever beam and a truss. Then, experimental validation is performed using a WSN and a cantilever beam.

2. Background

2.1 Modal identification using FDD

When monitoring in service civil engineering structures, the primary sources of external excitations are ambient vibrations such as those caused by wind or traffic loads. Because ambient excitation sources are often unmeasurable, only the resulting structural responses, the system outputs, can be reliably used for modal identification and damage detection. One effective method for output-only modal identification is the Frequency Domain Decomposition (FDD) method (Brinker *et al.* 2008). The FDD method is employed here for its speed and suitability for distributed computation in a WSN.

In the FDD method, the cross spectral density (CSD) function matrix relating responses at each discrete frequency is first estimated. To minimize the impact of measurement noise, the averaged CSD

matrix is obtained by performing an averaging operation on the CSD matrices estimated from multiple frames of data. Then a singular value decomposition (SVD) is performed on the averaged CSD matrix at each discrete frequency. The maximum singular value in each singular value matrix is collected to form a vector. From the peaks of this vector, structural natural frequencies are identified. The first column of the left singular decomposition matrix corresponding to a particular natural frequency is an estimate of the corresponding mode shape. In the implementation discussed herein, because only output information is used for identification the identified results from the FDD method are actually operational deflection shapes (OPS).

2.2 Flexibility-based damage detection

Techniques for damage detection based on structural flexibility have been gaining attention. A good estimate of the flexibility matrix can be obtained with easily identified low-frequency modes, making them attractive for civil engineering applications. Also, the flexibility matrix corresponding to the sensor coordinates can be extracted directly from the matrices of system realization. For these reasons, and due to their success in prior studies (Pandey and Biswas 1995, Bernal and Gunes 2004, Gao and Spencer 2002), flexibility-based methods are employed in this study.

Based on the assumption that the presence of damage in structures reduces structural stiffness, and thus increases structural flexibility, the change in structural flexibility between the pre- and post-damaged states can be used to detect damage, which is the fundamental basis of the classical flexibility difference method (Pandey and Biswas 1995). Because the damage detection results using classical flexibilities are embodied as nodal or DOF's (degree of freedom) characterization, the classical flexibility difference method cannot directly localize damage to exact elements. Consequently, the ASH flexibility-based method (Yan *et al.* 2008) was proposed for localizing damage in beam-like structures. This method determines the change in Angles-between-String-and-Horizon (ASHs) of beam elements caused by damage, and thus it can localize damage to exact elements. The ASH flexibility matrix can be constructed as

$$\mathbf{F}_\theta = \sum_{r=1}^n \frac{1}{\omega_r^2} \mathbf{R}_r \mathbf{R}_r^T \quad (1)$$

where ω_r is the r th circular modal frequency; n is the number of modes used; \mathbf{R}_r is called the r th ASH mode shape, which can be expressed in terms of the r th translational mode shape as

$$\mathbf{R}_r = \left[\frac{1}{l_1} \varphi_{1,r} \quad \frac{1}{l_2} (\varphi_{2,r} - \varphi_{1,r}) \quad \cdots \quad \frac{1}{l_i} (\varphi_{i,r} - \varphi_{i-1,r}) \quad \cdots \quad \frac{1}{l_n} (\varphi_{n,r} - \varphi_{n-1,r}) \right]^T \quad (2)$$

where $\varphi_{i,r}$ denotes the i th component of the r th mode shape, and l_i denotes the length of the i th beam element. The components in the r th column of this flexibility matrix represent the ASHs of all beam elements of the structure resulting from a unit moment applied at two nodes of element r , with no force or moment on the other elements. Thus, the components in the ASH flexibility are associated with beam-elements of the beam's finite element model rather than nodes.

The maximum absolute values of the components in each column or the diagonals in the difference of ASH flexibility matrices between the pre- and post-damaged structures are extracted as damage indicators. By observing a "step and jump" in the plot of damage indicators versus element numbers, the damage locations are determined.

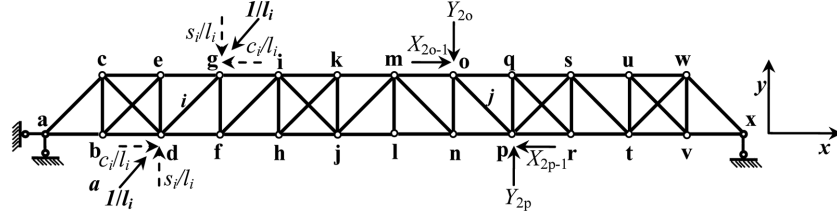


Fig. 1 Truss structure

To perform damage localization at the member-level in truss or frame structures, the Axial Strain (AS) flexibility-based method was proposed (Yan *et al.* 2009). The physical meaning of the AS flexibility is as follows: the components of the r th column of this flexibility matrix represent the axial strains of all elements or members resulting from a pair of axial forces with equal amplitudes, which are equal to the reciprocals of the length of the r th member, but acting in opposite directions at two nodes of the r th member. The basic idea is that if members in a structure are dominated by axial forces, as in truss structures, the axial strain will be a better index than deflection for damage detection.

The AS flexibility matrix is best explained through an example. For the truss in Fig. 1, the AS flexibility matrix is assembled as

$$\text{ASF} = \sum_{r=1}^n \frac{1}{\omega_r^2} \mathbf{S}_r \mathbf{S}_r^T \quad (3)$$

where

$$\mathbf{S}_r = \begin{pmatrix} c_1 \frac{(\varphi_{2a-1,r} - \varphi_{2b-1,r})}{l_1} + s_1 \frac{(\varphi_{2a,r} - \varphi_{2b,r})}{l_1} \\ \vdots \\ c_j \frac{(\varphi_{2o-1,r} - \varphi_{2p-1,r})}{l_j} + s_j \frac{(\varphi_{2o,r} - \varphi_{2p,r})}{l_j} \\ \vdots \\ c_n \frac{(\varphi_{2w-1,r} - \varphi_{2x-1,r})}{l_n} + s_n \frac{(\varphi_{2w,r} - \varphi_{2x,r})}{l_n} \end{pmatrix} \quad (4)$$

\mathbf{S}_r is called the r th axial strain mode shape and its j th component $c_j \frac{(\varphi_{2o-1,r} - \varphi_{2p-1,r})}{l_j} + s_j \frac{(\varphi_{2o,r} - \varphi_{2p,r})}{l_j}$ is associated with the j th member of the structure. l_j and $\varphi_{2p,r}$ denote the length of the j th member and the $2p$ component of the r th mode shape, respectively, and c_j and s_j denote the cosine and sine of the angle between the j th member and the x -axis in the global coordinate system.

The percent change in diagonal elements of the AS flexibility matrices before and after damage is taken as the damage indicators for each element. The elements associated with large values of damage indicators are identified as damaged.

In the original definition of the ASH or AS flexibility-based method, the mode shapes are required to be mass-normalized (Yan *et al.* 2008, 2009). However, the unit-length normalization of mode shape vectors is also working for their application. It is equivalent that the mass matrix is assumed to be an identity matrix. If the mass of a structure is really distributed uniformly along the structure, the

obtained flexibility is actually proportional to the real flexibility, and the proportional coefficient is an element in the mass matrix. In addition, considering that the identified mode shapes by the FDD method are operational deflection shapes (ODS), the ASH or AS flexibility constructed from the ODSs and/or non-normalized modes are actually pseudo-ASH or AS flexibility. In the sequel, "pseudo" is omitted.

3. Distributed computation strategy

In this section, the FDD method is modified to reduce computational efforts, and the way in which the modified FDD method and flexibility-based damage detection methods are distributed throughout a WSN is discussed to reduce the wireless communication amount to make effective use of energy in each sensor node.

A variation on the traditional FDD method is proposed here. Rather than performing a SVD on each of the CSD matrices at all discrete frequencies, a method with minimal computational efforts, peak-picking, is applied first to identify the natural frequencies. Then, noting that only the left singular decomposition matrices associated with the identified natural frequencies are used for obtaining mode shapes, we perform a SVD on each of the CSD matrices associated with those natural frequencies. And accordingly, we will just construct the CSD matrices associated with natural frequencies. In this way, the computational cost of identifying modal parameters is reduced considerably.

To construct the CSD matrices associated with natural frequencies under a WSN, we need to calculate the value of the CSD at each natural frequency for every pair of responses. Because the FFT of each response is obtained independently at each leaf node when using a distributed approach, we must relate the spectral responses at each leaf node. In addition, note that an averaged CSD matrix at a particular discrete frequency is only related to the CSD matrices associated with this discrete frequency obtained from different frames of data. Therefore, only the spectral responses associated with the natural frequencies (instead of the time-history responses) must be transmitted to a common sensor node (a cluster head here) in the WSN. Thus, the amount of wireless communication is reduced considerably.

FDD is combined with peak-picking herein to identify the modal parameters. First, on the microprocessor of each leaf node, a fast Fourier transform (FFT) is performed on a frame of data collected at each sensor node as

$$X_i(\omega) = F[x_i(t)] \quad (5)$$

where $F[\cdot]$ represents the FFT operation. $X_i(\omega)$ is the FFT coefficient of the response $x_i(t)$ at the i th node. Second, the auto-spectrum of each response is calculated as

$$P_i(\omega_j) = X_i(\omega_j)X_i^*(\omega_j) \quad (6)$$

where $P_i(\omega_j)$ denotes the power spectral density (PSD) function at the j th discrete frequency of $x_i(t)$. To improve the results, several frames of data are captured and an averaged PSD is calculated. Then, the peaks of the averaged PSD of $x_i(t)$ are identified for determining the natural frequencies using that the assumption that the external excitations considered here are broadband ambient vibrations. For automated identification, one would provide appropriate frequency values to bound the searching range for each of the peaks. Here we use ω_p to represent the discrete frequencies associated with the identified

p th peak. This step is also performed independently at each leaf node. However, not all peaks are necessarily related to natural frequencies of the system. A discussion of some practical issues associated with this step is provided in the sequel.

From each leaf node, only the resulting discrete frequencies ω_p and the FFT coefficients $X_i(\omega_p)$ corresponding to the peaks (from an FFT of each frame of data) are transmitted to a cluster head. Obviously, this significantly reduces the amount of data to be transmitted compared with transmitting the entire time history.

The remaining steps involved in modal identification are performed at the cluster head. After the cluster head receives a set of intermediate results obtained from one frame of data from each leaf node, the CSD between each response and a reference response (the response at the cluster head is taken as the reference response here) is calculated to determine if each discrete frequency ω_p is a structural frequency. To judge this, the phase of the CSD is examined. For a discrete frequency ω_p , if the phase of the corresponding CSD at $\omega = \omega_p$ is close to 0 or π , the discrete frequency ω_p is a natural frequency of the structure (designated ω_n). Using this criterion, the natural frequencies can be identified with the intermediate results.

Then, for this frame of data, the CSD matrix corresponding to each natural frequency is estimated from the FFT coefficients associated with the identified natural frequencies ω_n (instead of ω_p). It is worth noting that, when calculating each CSD matrix, the FFT coefficients must originate from the same frame of response data for all DOFs. The estimated CSD matrix corresponding to the k th natural frequency ω_n^k is expressed as

$$\mathbf{G}(\omega_n^k) = \begin{bmatrix} X_1(\omega_n^k)X_1^*(\omega_n^k) & \cdots & X_1(\omega_n^k)X_i^*(\omega_n^k) & \cdots & X_1(\omega_n^k)X_n^*(\omega_n^k) \\ \vdots & & \vdots & & \vdots \\ X_i(\omega_n^k)X_1^*(\omega_n^k) & \cdots & X_i(\omega_n^k)X_i^*(\omega_n^k) & \cdots & X_i(\omega_n^k)X_n^*(\omega_n^k) \\ \vdots & & \vdots & & \vdots \\ X_n(\omega_n^k)X_1^*(\omega_n^k) & \cdots & X_n(\omega_n^k)X_i^*(\omega_n^k) & \cdots & X_n(\omega_n^k)X_n^*(\omega_n^k) \end{bmatrix} \quad (7)$$

After the intermediate results obtained from various frames of data are transmitted to the cluster head, the average value of identified natural frequencies from all leaf nodes and from all various frames of data is calculated to obtain the final identified natural frequency for each mode. The averaged CSD matrix associated with each natural frequency (designated $\bar{\mathbf{G}}(\omega_n^k)$) is obtained by performing an average on $\mathbf{G}(\omega_n^k)$ estimated from various frames of data. Next, a SVD is performed on each of the averaged CSD matrices corresponding to each natural frequency to identify the associated mode shapes

$$\mathbf{U}\Sigma V^T = SVD(\bar{\mathbf{G}}(\omega_n^k)) \quad (8)$$

where Σ , \mathbf{U} and V denote the singular value matrix, the left singular decomposition matrix and the right singular decomposition matrix.

The first column of \mathbf{U} is an estimate of the k th mode shape (actually, ODS) and is designated \mathbf{U}_1 . By dividing all of the components of \mathbf{U}_1 by the component of \mathbf{U}_1 chosen as a reference, the normalized ODS is obtained with one component having a value of one. Its components are, in general, complex values. The phase associated with each complex value represents the phase difference between that response location and the reference sensor location in the k th mode. To obtain the real-valued components of the ODS, which are typically used for damage detection, the magnitude of each component

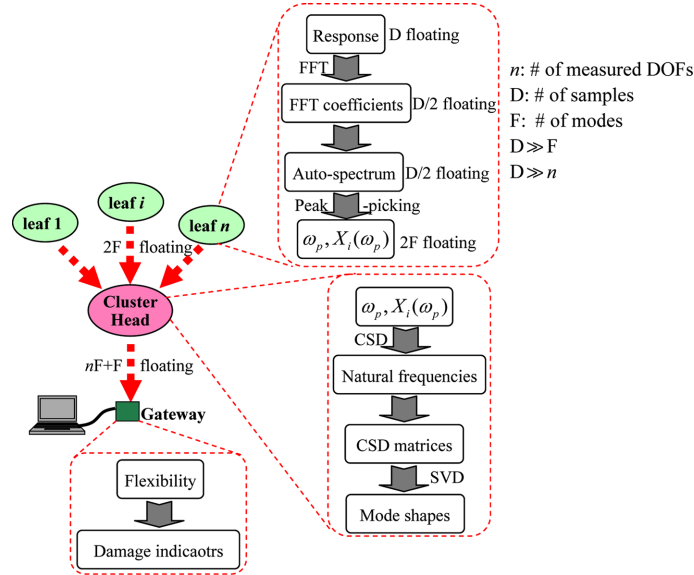


Fig. 2 The distribution of system identification and damage detection across the WSN and the data flow between stages

of the normalized U_1 is calculated. The corresponding sign for each component is determined by its respective phase. The phases of the components in the normalized ODS are ideally equal to 0 or π for proportionally damped systems with no measurement error. In practice, due to measurement and numerical errors, the phases are not exactly 0 or π . The signs of the components are determined as follows (as in the original FDD method): if the phase is in the range of $[-\frac{\pi}{2}, \frac{\pi}{2}]$, the corresponding sign is positive; otherwise, if the phase is in the range of $[\frac{\pi}{2}, \frac{3\pi}{2}]$, the corresponding sign is negative.

Once natural frequencies and ODSs are obtained at the cluster head, they are transmitted to the gateway mote of the PC base station. The amount of data to be transferred here is also small compared to transmitting the entire time history. All the procedures of damage detection are performed at the gateway mote. First, the identified natural frequencies and ODSs are applied to construct a flexibility matrix. Then, damage indicators are extracted from the difference between the flexibility matrix in the current state and the flexibility matrix constructed from the baseline data stored in the gateway mote (details will be provided in Section 4), and are transmitted to the PC base station through a USB cable.

The distribution of the modified FDD method and damage detection methods across the WSN and the data flow between stages are shown in the flowchart in Fig. 2. Herein, it is assumed that the number of modes to be identified is F , and each data frame has D sampling points, and the number of points in the FFT is D . The amount of data transmitted from each leaf node to the cluster head is $2F$ floating, and the amount of data transmitted from the cluster head to the gateway mote is $(n+1)F$ floating. Both are much smaller than D .

In summary, in this modified FDD method, the SVD is performed on only a few matrices (the number is equal to the number of the identified natural frequencies), therefore the computing efforts at the cluster head are reduced significantly as compared with the original FDD method without sacrificing accuracy in the identified ODSs. In addition, using the distributed computation strategy, only small

amount of data is transmitted wirelessly, which subsequently alleviates the issues related to the limited power supply in WSNs.

4. Multi-level damage localization implementation

As described in Section 2, the distributed computation of modal identification and damage detection is able to reduce the energy consumption of a sensor node while it is awake. However, allowing many of the sensors to remain asleep required much less energy than that used to keep them active (Polastre *et al.* 2005). To take advantage of this feature, we propose a multi-level damage localization strategy to further reduce the total energy consumption in a WSN by activating relatively few sensors and allowing unused sensors to be in a sleep mode. Thus, although a large number of wireless sensors are installed in a structure, only some of them are activated at the first level and the information measured from them is used to localize damage to larger regions. Once this is done, more sensors in the damaged regions are then activated to generate a new network to perform finer-grained damage localization. The ASH flexibility-based method is identified for level-1 damage localization. This approach can locate a damage site between two measurement sensors when measured DOFs are not complete (Castaneda *et al.* 2008). For level-2 damage localization, different methods may be used for different types of structures.

For beam structures, the procedures to perform multi-level damage localization are as follows. When the wireless sensor network is first turned on, a baseline modal identification is performed. All sensor nodes are activated here. First, they are synchronized and acquire structural responses. Then, the acquired data is resampled to make all the responses have the same sampling frequency, perform FFT on the resampled response, pick peaks in the PSD of responses and transmit some intermediate results to a cluster head. Next, the natural frequencies and ODSs are identified at the cluster head and are transmitted to the gateway mote connected to the base station. Finally, the baseline data are stored in the gateway mote as constant parameters for a particular structure.

After the baseline modal identification is performed, the level-1 damage localization begins operating with only a few sensors activated. The data acquisition and modal identification above are repeated on these activated sensors. Then, an ASH flexibility matrix for the current state is constructed using the identified natural frequencies and ODSs. Meanwhile, a baseline flexibility matrix is constructed using natural frequencies and the associated ODS components with sensors activated, which are already stored in the gateway mote of the base station. By extracting the damage indicators from the flexibility difference matrix between the current state and the baseline, the gateway mote can determine automatically if the structure is damaged. If no damage is detected, the search ends and all the sensor nodes return to sleep until the next damage detection period comes. If damage is detected, the gateway mote will provide the information on damaged regions which are used for instructions of activating more sensors, and the level-2 damage localization will be automatically initiated.

For the level-2 damage localization, more sensors in potentially damaged regions are awakened and added to the network. The data acquisition and modal identification above are repeated on the new network. The ASH flexibility-based method is performed with an increase in the spatial resolution of sensors near the damage. Therefore, the second round can subsequently localize damage to a smaller region than the first round. This network may repeat this drill-down procedure to achieve even finer-grained results until the desired resolution is reached. The multi-level damage localization strategy with distributed computation is illustrated using an example in Fig. 3.

Let us take a bridge as an example to illustrate this proposed strategy, as shown in Fig. 3. Assume

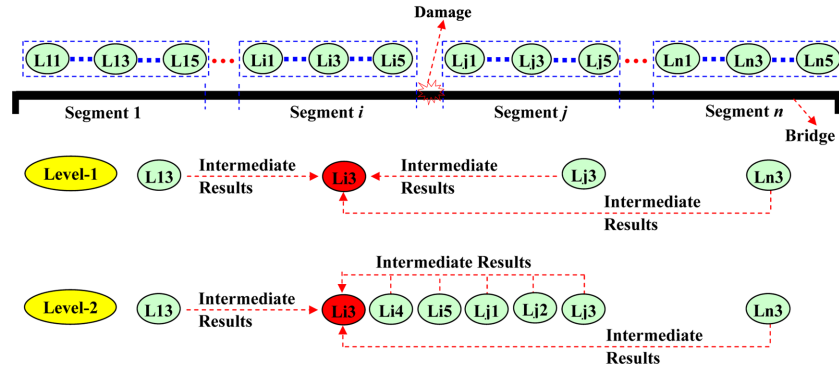


Fig. 3 Network architecture for multi-level damage localization strategy with distributed computation

that we deploy five wireless sensors on each segment of the bridge. At the first stage, we just activate one sensor in each segment. These sensors form one network. One sensor (with red background) is used as a manager, called as a cluster head, and the others are their subordinates, called as leaf nodes. At each leaf node, after sensing the response, the sensor does not transmit the acquired data to the cluster head or base station directly, but rather process the response onboard each sensor node and only some useful intermediate results are transmitted wirelessly to the cluster head. Using the current WSN, damage can be localized between L_{i3} and L_{j3} . To further localize damage, the leaf nodes between L_{i3} and L_{j3} are activated and added to the network to form a new network. Performing the same procedures as above, the damage will be localized to a smaller region, between L_{i5} and L_{j1} .

For truss structures, the procedures for performing multi-level damage localization are similar to those used for beam structures. The only difference lies in that: 1) the ASH flexibility-based method is used to perform bay-level damage localization (level-1), by considering a truss as a beam, and 2) the AS flexibility-based method is used to perform member-level damage localization (level-2). Using this approach, many nodes in the WSN remain asleep for part or all of the implementation, reducing the total energy usage significantly.

5. Illustrative examples

5.1 Cantilever beam

To demonstrate the performance of the proposed strategy numerically, a cantilever beam is first considered. This beam is assumed to be made of aluminum with dimensions 2080 mm×20 mm×20 mm. Young’s modulus, the mass density and Poisson’s ratio of the material are 70 Gpa, 2700 kg/m³ and 0.3, respectively. The beam is modeled using 26 beam elements, each of 80 mm long, with 27 nodes, as shown in Fig. 4 ($n = 26$ here). The first four analytical natural frequencies of this beam are shown in Table 1.

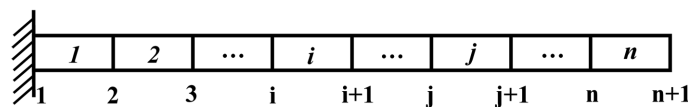


Fig. 4 Cantilever beam with discrete elements

Table 1 Natural frequencies of cantilever beam before and after damage (Hz)

	Analytical		Identified		Percentage change of identified results (%)
	Intact	Damaged	Intact	Damaged	
1	3.80	2.96	3.66	3.09	15.57
2	23.73	22.09	23.91	21.94	8.24
3	66.15	57.98	66.09	57.94	12.33
4	128.92	109.09	129.38	109.13	15.65

Proportional viscous damping is included with a damping ratio of 1% in each mode of the structure. Independent band-limited white noise processes are applied vertically at all nodes to simulate ambient vibration. Acceleration responses in the vertical direction are obtained in the simulation, and measurement noise is simulated by adding independent, zero-mean white noise processes with an RMS of 5% of the responses to these values. The responses are recorded at 1152 Hz.

Damage is simulated in this example as a reduction in the stiffness of some elements in the model, by assuming a 50% reduction in the cross-sectional area in elements 4 and 22. The first four natural frequencies identified in the damaged case are shown in Table 1. We use a 50% reduction in the area because this is representative of our experimental test and the testing restrictions therein (as shall be shown in Section 6). Actually, in simulation this method has been successful in localizing damage with only a 10% reduction (Yan *et al.* 2008).

For purposes of this example, assume that one wireless sensor is placed at each node of the model. First, for level-1 implementation, we uniformly activate a smaller number of wireless sensors to locate potentially damaged regions. Assume that seven sensors (at nodes 3, 7, 11, 15, 19, 23 and 26) are activated and only vertical responses associated with these nodes are acquired. The computing-distributed FDD method is used to identify modal parameters. The first four identified modes are used to construct the ASH flexibility matrices before and after damage. The damage indicators are plotted in Fig. 5. From the “step and jump” distribution of damage indicators, it is clear that damage occurs near nodes 3 and 23.

To further localize the damage, those sensors in the two damaged regions are activated and added to the network for a level-2 implementation. The data measured in this configuration are the responses at nodes 1 through 6, 10, 14 and 18 through 26 (17 responses in total). Fig. 6 presents damage indicators based on the ASH flexibility when more sensors are activated. The damage indicators associated with

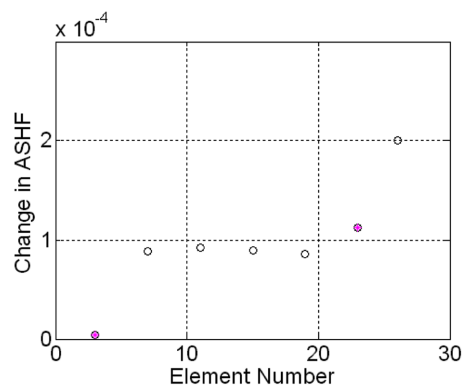


Fig. 5 Level-1 damage localization results for cantilever beam using ASH flexibility-based method with seven measurement points

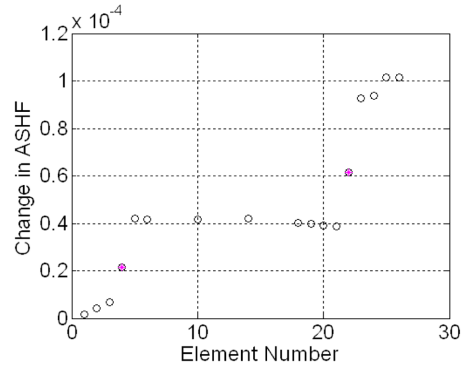


Fig. 6 Level-2 damage localization results for cantilever beam using ASH flexibility-based method with 17 measurement points

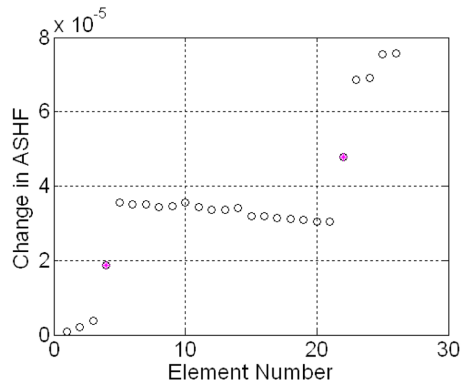


Fig. 7 Damage localization results for cantilever beam using ASH flexibility-based method with all measurement points

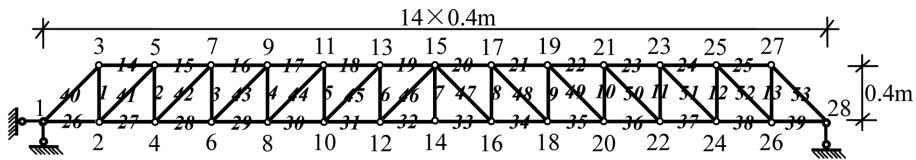


Fig. 8 14-bay planar truss

elements 4 and 22 exhibit as jumps between two steps. It suggests that we successfully localize the damage to elements 4 and 22 in level-2. The damage location results using all nodal responses are shown for comparison in Fig. 7. Clearly, using the proposed strategy, damage localization results with enough accuracy are obtained with relatively few sensors.

5.2 Planar truss

In a second example we consider a 14-bay planar truss structure simply supported at the ends (see Fig. 8). The cross-sectional area of each member is $1.122 \times 10^{-4} \text{ m}^2$. Young's modulus, the mass density and Poisson's ratio of the material are $2 \times 10^{11} \text{ Pa}$, 7850 kg/m^3 and 0.3, respectively. The finite element model (FEM) has 28 nodes and 53 members. The numbering of elements and nodes of the FEM is

Table 2 Natural frequencies of truss before and after damage (Hz)

	Analytical		Identified		Percentage change of identified results (%)
	Intact	Damaged	Intact	Damaged	
1	8.57	7.95	8.72	7.88	9.63
2	29.00	26.68	28.97	26.72	7.77
3	42.74	40.44	42.75	40.50	5.26
4	57.92	54.46	57.66	54.28	5.86

shown in Fig. 8. Lumped masses of 0.5 kg are included at the 1st and 28th nodes, and 10 kg are included on all other nodes. The first four analytical natural frequencies are listed in Table 2.

Simulation of the modal experiment is similar to that of the prior numerical example. Independent band-limited white noise processes are applied in the horizontal direction and the vertical direction at all nodes to excite the structure. The simulated sampling frequency is 560 Hz. Measurement noise is also added to the response at each node.

Damage is simulated as a 50% reduction in the cross-sectional areas of the following members: members 16, 43 and 29 in the 4th bay, and members 9, 22, 49 and 35 in the 10th bay.

In the multi-level approach on the truss, we try to first localize damage to the bays. For this step, the truss is viewed as a beam with 14 elements. Only the vertical responses of nodes along the lower chords are used to identify the modal parameters. The identified natural frequencies are listed in Table 2. The ASH flexibility-based method is employed to perform the bay-level (level-1) damage localization. The first two modes are used to assemble the ASH flexibility. The extracted damage indicators are presented in Fig. 9. The damage indicators corresponding to bays 4 and 10 exhibit as jumps between steps, which suggests that damage occurs near the 4th and 10th bays.

To further localize damage to exact members, assume that the sensors around the 4th and the 10th bays are activated (at nodes 4 through 11, and at nodes 16 through 23). The AS flexibility-based method is used and the responses measured by the recently activated sensors are used for the computing-distributed FDD method to identify modal parameters. The first two modes are used to construct the AS flexibility matrices before and after damage. The extracted damage indicators are plotted in Fig. 10. The maxima among the damage indicators suggest that the AS flexibility-based method successfully identifies all the damaged members (members 9, 16, 22, 29, 35, 43 and 49).

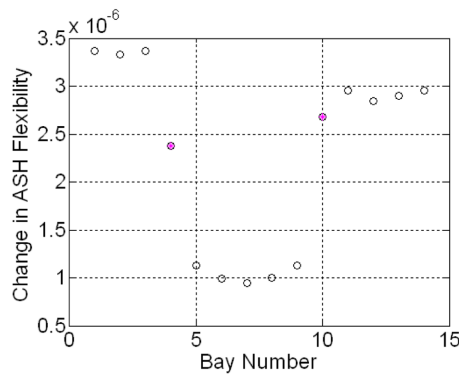


Fig. 9 Level-1 damage localization results for truss using ASH flexibility-based method

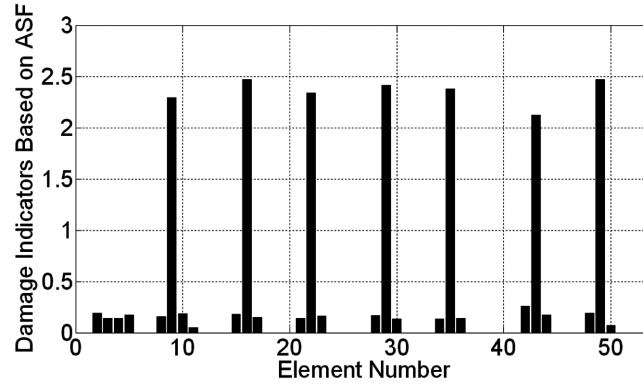


Fig. 10 Level-2 damage localization results for truss using AS flexibility-based method

6. Experimental validation

To experimentally validate the proposed approach, we deploy a network of Imote2 (Crossbow Technology) wireless sensor platforms and associated sensor boards. The modified FDD method and the two flexibility-based damage detection methods are implemented on top of the TinyOS 1.1 operating system (<http://www.tinyos.net>) using the nesC programming language. Our implementation leverages several existing SHM middleware services developed at UIUC (<http://shm.cs.uiuc.edu/>), namely, their enhanced sensor driver, a reliable data transmission network layer, and an implementation of the FTSP time synchronization protocol (Maróti *et al.* 2004) used for time-synchronizing the responses measured from different sensors. Procedures executed in the proposed system at the leaf nodes, cluster heads and the gateway mote of the base station are listed in the respective blocks in Fig. 3.

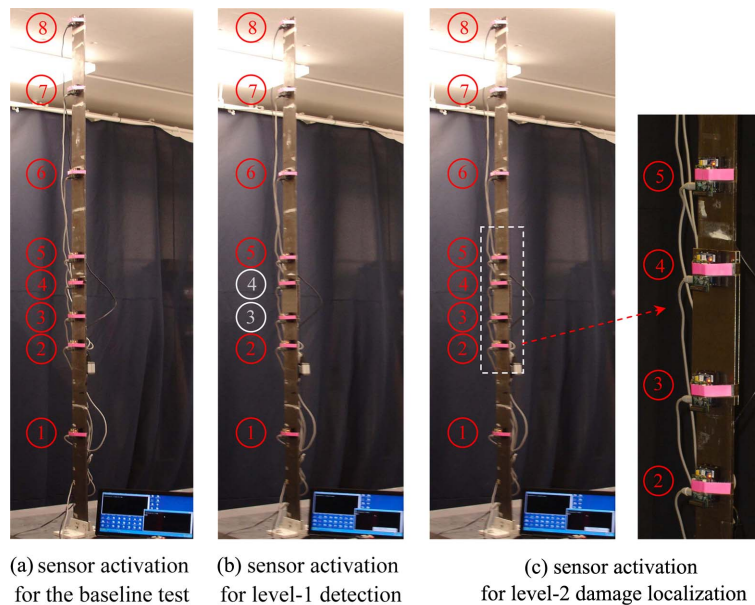


Fig. 11 The cantilever beam and sensor placements in the experiment tests

Experimental validation tests are conducted using a steel cantilever beam at the Structural Control and Earthquake Engineering Lab at Washington University. The beam is 108 in long, 3 in wide and 0.25 in thick, as shown in Fig. 11. The sensor numbers are shown in the circles in each figure. The beam is fixed to the shake table in a vertical position. Damage in the beam is simulated by adding a pair of thin, symmetric steel plates in element 4. These plates are 9 in long, 3.625 in wide and 0.0625 in thick.

In these tests, the SHM system includes a PC base station, eight Intel Imote2 motes (IPR2400) with sensor boards (ITS400C), and a “gateway” Imote2 board tethered to the base station with a PC interface board (IIB2400). Each Imote2 board is equipped with 256 KB of integrated SRAM and 32 MB of external SDRAM, an XScale CPU capable of running at speeds up to 614 MHz, an 802.15.4-compliant radio (CC2420) and a 2.4 Hz antenna (Crossbow Technology). Sensors are deployed along the beam, as shown in Fig. 11. In this experiment, all sensors are within a single hop from the base station. All modal identification and damage detection procedures are automated on the sensors. The damage indicators are extracted at the gateway mote connected to the base station.

The beam is excited along the weak axis of bending using an impact. The acceleration response in this direction is collected at each node. For data collection, the sampling frequency of acceleration response is 280 Hz, the length of record is 7168 points, and the number of points in the FFT is 2048.

First, we run the developed WSN-based SHM system on the intact beam to obtain baseline modal parameters. These values are saved on the gateway mote connected to the base station. For purposes of code validation, a file is generated containing the obtained baseline data, the identified natural frequencies (as shown in Table 3) and ODSs (as shown in Fig. 12).

Then, we deploy the WSN-based SHM system on the damaged beam. The gateway mote extracts the damage indicators automatically, and identifies if the beam is damaged and when to initiate the level-2 damage localization. For level-1 damage localization, only six sensor nodes (nodes 1, 2, 5 through 8) are activated. The extracted damage indicators at the gateway mote are plotted in Fig. 13(a). The damage indicator associated with element 3 exhibits a peak, which means the damage is localized to element 3 (corresponding to the current network architecture). Then, the system automatically

Table 3 Identified natural frequencies of the cantilever beam before and after damage

Order	Intact (Hz)	Damaged (Hz)	Percentage change (%)
1	0.5469	0.5469	0
2	3.9648	3.9648	0
3	11.1454	11.2109	0.59

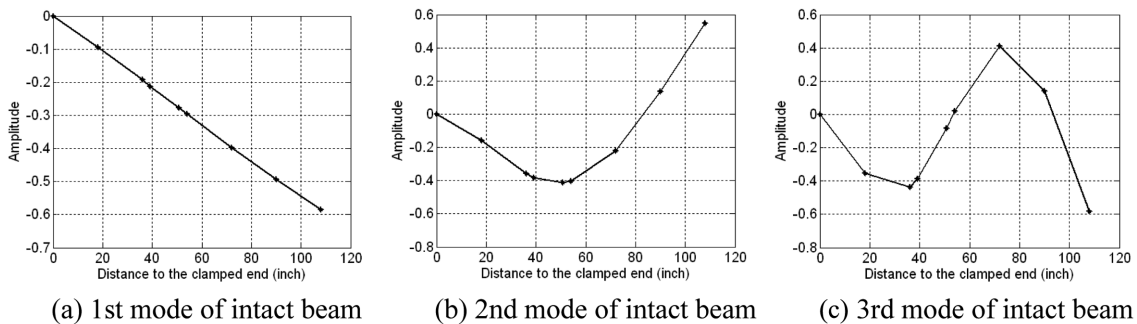


Fig. 12 Identified ODSs of the intact beam

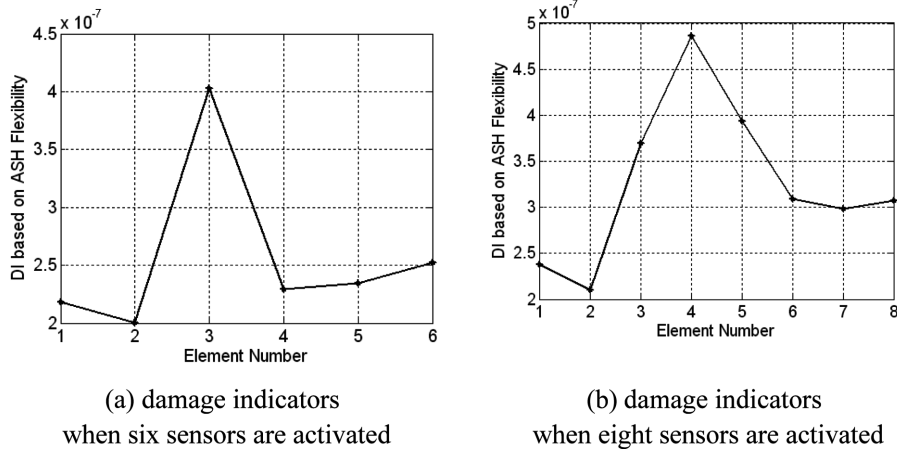


Fig. 13 Damage localization results using the developed WSN-based SHM system

activates two more sensors within element 3 and performs level-2 detection. The damage indicators extracted by the system are plotted in Fig. 13(b). From the peak among the damage indicators, we can localize damage to a smaller region (element 4 in the new network architecture) which is consistent with the position of the two steel plates.

7. Conclusions

A multi-level damage localization strategy suitable for implementation on a WSN using a distributed computation is proposed in this paper. A variation of the FDD method is employed for modal identification, and the damage detection step is based on a computed flexibility matrix. The implementation is designed to consume minimal energy. Using the distributed computation strategy, the acquired responses are processed at the sensor nodes and only a small amount of intermediate results are transmitted, reducing the energy consumed on each leaf node. Furthermore, using the proposed multi-level damage localization strategy, most of the nodes are able to remain asleep for part or all of the interrogations, reducing the total energy consumed. Numerical simulations and experimental tests were successfully conducted to validate the effectiveness of the proposed strategy.

Acknowledgments

The authors acknowledge the support of the US National Science Foundation through Grant Nos. 0625640 and NeTS-NOSS Grant CNS- 0627126. The authors also would like to acknowledge Professor Bill F. Spencer and his students (Jennifer Rice and Sung-Han Sim) in University of Illinois at Urbana-Champaign for providing some of the codes used in these studies. Additionally, the first author would like to acknowledge support of the National Natural Science Foundation of China under Grant No. 50708029.

References

- American Society of Civil Engineers (ASCE), (2009), *Report Card for America's Infrastructure*, Reston, Virginia, USA.
- Bernal, D. and Gunes, B. (2004), "Flexibility based approach for damage characterization: benchmark application", *J. Eng. Mech.*, **130**(1), 61-70.
- Brinker, R., Zhang, L. and Andersen, P. (2000), "Modal identification from ambient responses using frequency domain decomposition", *Proceedings of the 18th International Modal Analysis Conference*, San Antonio, TX.
- Castaneda, N., Dyke, S., Lu, C., Sun, F. and Hackmann, G. (2009), "Experimental deployment and validation of a distributed shm system using wireless sensor networks", *Struct. Eng. Mech.*, **32**(6), 787-809.
- Chintalapudi, K., Johnson, E.A. and Govindan, R. (2005), "Structural damage detection using wireless sensor-actuator networks", *Proceedings of the 13th MoM03-4 Mediterranean Conference on Control and Automation*, Limassol, Cyprus, June.
- Crossbow Technology, Inc., *ITS400 Imote2 Basic Sensor Board*, Available at http://www.xbow.com/Products/Product_pdf_files/Wireless_pdf/ITS400_Datasheet.pdf.
- Feng, J., Koushanfar, F. and Potkonjak, M. (2002), "System-architecture for sensor networks issues, alternatives, and directions", *Proceedings of the 2002 IEEE International Conference on Computer Design (ICCD '02)*.
- Galbreath, J.H., Townsend, C.P., Mundell, S.W., Hamel, M.J., Esser, B., Huston, D. and Arms, S.W. (2003), "Civil structure strain monitoring with power-efficient, high-speed wireless sensor networks", *Proceedings of the 4th Interantional Workshop on Structural Health Monitoring*, Stanford University, Stanford, CA, September.
- Gao, Y. and Spencer, B.F. (2002), "Flexibility-based damage location employing ambient vibration", *Proceedings of the 15th ASCE Engineering Mechanics Conference*, New York.
- Hackmann, G., Chipara, O. and Lu, C.Y. (2008), "Robust topology control for indoor wireless sensor networks", *Proceedings of the 6th ACM conference on Embedded network sensor systems*, Raleigh, NC, USA, November.
- Hackmann, G., Sun, F., Castaneda, N., Lu, C. and Dyke, S. (2008), "A holistic approach to decentralized structural damage localization using wireless sensor networks", *Proceedings of the 29th IEEE Real-Time Systems Symposium*, Barcelona, Spain, November.
- Horton, M.A., Glaser, S. and Sitar, N. (2002), "Wireless networks for structural health monitoring and hazard mitigation", *Proceedings of the US-Europe Workshop on Sensors and Smart Structures Technology*.
- Jason Lester, Hill (2003), *System Architecture for Wireless Sensor Network*, PhD Dissertation, University of California, Berkeley.
- Jeong, Min-Joong and Koh, Bong-Hwan (2009), "A decentralized approach to damage localization through smart wireless sensors", *Smart Struct. Syst.*, **5**(1), 43-54.
- Lynch, J.P., Kiremidjian, A.S., Law, K.H., Kenny, T. and Carryer, E. (2002), "Issues in wireless structural damage monitoring technologies", *Proceedings of the Third World Conference on Structural Control*, Como, Italy, April.
- Lynch, J.P., Sundararajan, A., Law, K.H., Kiremidjian, A.S. and Carryer, E. (2004), "Embedding damage detection algorithms in a wireless sensing unit for operational power efficiency", *Smart Mater. Struct.*, **13**(4), 800-810.
- Maróti, M., Kusy, B., Simon, G. and Lédeczi, A. (2004), "The flooding time synchronization protocol", *Proceedings of the 2nd International Conference on Embedded Network Systems*, Baltimore, Maryland, USA, November.
- Messina, A., Jones, I.A. and Williams, E.J. (1996), "Damage detection and localization using natural frequencies changes", *Proceedings of the Conference on Identification in Engineering Systems*, Swansea, UK.
- Moss, David and Levis, Philip (2008), *BoX-MACs: Exploiting physical and link layer boundaries in low-power networking*, Technical Report SING-08-00, Stanford Information Networks Group.
- Nagayama, T. and Spencer, Jr., B.F. (2007), *Structural Health Monitoring Using Smart Sensors*, Newmark Structural Engineering Laboratory (NSEL) Report Series, No.NSEL-001, University of Illinois, Urbana-Champaign, Available at <http://hdl.handle.net/2142/3521>.
- Pandey, A.K. and Biswas, M. (1995), "Experimental verification of flexibility difference method for locating damage in structures", *J. Sound Vib.*, **184**(2), 311-328.
- Polastre, J., Szewczyk, R. and Culler, D. (2005), "Telos: enabling ultra-low power wireless research", *Proceedings of the 4th international symposium on Information processing in sensor networks*, Piscataway,

- NJ, USA.
- Spencer, B.F. (2003), "Opportunities and challenges for smart sensing technology", *Proceedings of the First International Conference on Structural Health Monitoring and Intelligent Infrastructure*, Tokyo, November.
- Wang, Yang, Lynch, Jerome P. and Law, Kincho H. (2007a), "A wireless structural health monitoring system with multithreaded sensing devices: design and validation", *Struct. Infrastruct. E.*, **3**(2), 103-120.
- Wang, Yang, Swartz, R. Andrew, Lynch, Jerome P., Law, Kincho H., Lu, Kung-Chun and Loh, Chin-Hsiung (2007b), "Decentralized civil structural control using real-time wireless sensing and embedded computing", *Smart Struct. Syst.*, **3**(3), 321-340.
- Yan, Guirong, Duan, Zhongdong and Ou, Jinping (2008), "Structural damage detection using the angle-between-string-and-horizon flexibility", Submitted to *Struct. Eng. Mech.* and under review.
- Yan, Guirong, Duan, Zhongdong and Ou, Jinping (2009), "Damage detection for truss or frame structures using an axial strain flexibility", *Smart Struct. Syst.*, **5**(3), 291-316.
- Ye, Wei, Silva, Fabio and Heidemann, John (2006), "Ultra-low duty cycle MAC with scheduled channel polling", *Proceedings of the 4th international conference on Embedded networked sensor systems*, Boulder, Colorado, USA, November.
- Yu, Yan and Ou, Jinping (2009), "Wireless collection and data fusion method of strain signal in civil engineering structures", *Sensor Review*, **29**(1), 63-69.
- Yu, Yan, Ou, Jinping, Zhang, Jun, Zhang, Chunwei and Li, Luyu (2009), "Development of wireless MEMS inclination sensor system for swing monitoring of large scale hook structures", *IEEE T. Ind. Electron.*, **56**(4), 1072-1078.
- Zimmerman, A.T., Shiraishi, M., Swartz, R.A. and Lynch, J.P. (2008), "Auto-mated modal parameter estimation by parallel processing within wireless monitoring systems", *J. Infrastruct. Syst.*, **14**, 102-113.